

University of Groningen

Comparison of the uptake mechanisms of zwitterionic and negatively charged liposomes by HeLa cells

Montizaan, Daphne; Yang, Keni; Reker-Smit, Catharina; Salvati, Anna

Published in:
Nanomedicine-Nanotechnology biology and medicine

DOI:
[10.1016/j.nano.2020.102300](https://doi.org/10.1016/j.nano.2020.102300)

IMPORTANT NOTE: You are advised to consult the publisher's version (publisher's PDF) if you wish to cite from it. Please check the document version below.

Document Version
Publisher's PDF, also known as Version of record

Publication date:
2020

[Link to publication in University of Groningen/UMCG research database](#)

Citation for published version (APA):
Montizaan, D., Yang, K., Reker-Smit, C., & Salvati, A. (2020). Comparison of the uptake mechanisms of zwitterionic and negatively charged liposomes by HeLa cells. *Nanomedicine-Nanotechnology biology and medicine*, 30, [102300]. <https://doi.org/10.1016/j.nano.2020.102300>

Copyright

Other than for strictly personal use, it is not permitted to download or to forward/distribute the text or part of it without the consent of the author(s) and/or copyright holder(s), unless the work is under an open content license (like Creative Commons).

The publication may also be distributed here under the terms of Article 25fa of the Dutch Copyright Act, indicated by the "Taverne" license. More information can be found on the University of Groningen website: <https://www.rug.nl/library/open-access/self-archiving-pure/taverne-amendment>.

Take-down policy

If you believe that this document breaches copyright please contact us providing details, and we will remove access to the work immediately and investigate your claim.

Downloaded from the University of Groningen/UMCG research database (Pure): <http://www.rug.nl/research/portal>. For technical reasons the number of authors shown on this cover page is limited to 10 maximum.



ELSEVIER



BASIC SCIENCE

Nanomedicine: Nanotechnology, Biology, and Medicine
30 (2020) 102300



nanomedjournal.com

Original Article

Comparison of the uptake mechanisms of zwitterionic and negatively charged liposomes by HeLa cells^{*}

Daphne Montizaan, MSc¹, Keni Yang, PhD¹, Catharina Reker-Smit, Ing, Anna Salvati, PhD^{*}

Department of Nanomedicine & Drug Targeting, Groningen Research Institute of Pharmacy, University of Groningen, Groningen, The Netherlands

Revised 28 August 2020

Abstract

Zwitterionic molecules are used as an alternative to PEGylation to reduce protein adsorption on nanocarriers. Nonetheless, little is known on the effect of zwitterionic modifications on the mechanisms cells use for nanocarrier uptake. In this study, the uptake mechanism of liposomes containing zwitterionic or negatively charged lipids was characterized using pharmacological inhibitors and RNA interference on HeLa cells to block endocytosis. As expected, introducing zwitterionic lipids reduced protein adsorption in serum, as well as uptake efficiency. Blocking clathrin-mediated endocytosis strongly decreased the uptake of the negatively charged liposomes, but not the zwitterionic ones. Additionally, inhibition of macropinocytosis reduced uptake of both liposomes, but blocking actin polymerization had effects only on the negatively charged ones. Overall, the results clearly indicated that the two liposomes were internalized by HeLa cells using different pathways. Thus, introducing zwitterionic lipids affects not only protein adsorption and uptake efficiency, but also the mechanisms of liposome uptake by cells.

© 2020 The Author(s). Published by Elsevier Inc. This is an open access article under the CC BY license (<http://creativecommons.org/licenses/by/4.0/>).

Key words: Zwitterionic; Liposome; Uptake mechanism; Pharmacological inhibitor

Nanomedicine holds great potential for improving the ways drugs are delivered to their targets. Nanocarriers can be used to direct drugs to the diseased tissue, and promote their internalization into the targeted cells.^{1–3} Although the successes of this technology have confirmed nanomedicine potential, drug targeting still constitutes a major challenge in nanomedicine and more work is required to further improve current outcomes.^{3–6}

One of the challenges in targeting nanomedicines is the adsorption of proteins and other biomolecules on their surface, forming a corona once they are applied in biological

environments.^{7,8} Protein adsorption and corona formation are usually associated with recognition by the immune system and clearance of nanocarriers from the systemic circulation.^{9–12} Corona formation can also affect the targeting ability of nanomedicines by masking targeting moieties on the nanocarrier.^{13,14} At the same time, corona proteins can interact with specific cell receptors and facilitate or hamper nanocarrier uptake by cells.^{15–17} The composition of the corona depends on the biological environment and the physicochemical properties of the nanocarrier, thus changing nanocarrier design can affect

Abbreviations: DOPC, 1,2-dioleoyl-sn-glycero-3-phosphocholine; DOPG, 1,2-dioleoyl-sn-glycero-3-phospho-(1'-rac-glycerol); SRB, sulforhodamine B; CD47, cluster of differentiation 47; PBS, phosphate buffered saline; MWCO, molecular weight cut off; MEM, minimum essential medium; hsMEM, MEM medium supplemented with 4 mg/mL human serum; FBS, fetal bovine serum; cMEM, complete MEM medium supplemented with 10% FBS; sMEM, serum-free MEM; SEC, size exclusion chromatography; SDS-PAGE, sodium dodecyl sulfate–polyacrylamide gel electrophoresis; EIPA, 5-(N-ethyl-N-isopropyl)amiloride; MβCD, methyl-β-cyclodextrin; LDL, low-density lipoprotein; EDTA, ethylenediaminetetraacetic acid; TRITC, tetramethylrhodamine; DAPI, 4',6-diamidino-2-phenylindole; DLS, dynamic light scattering; CME, clathrin-mediated endocytosis; DNM, dynamin; GTPase, guanosine triphosphatase; Rac1, Ras-related C3 botulinum toxin substrate 1; Cdc42, cell division control protein 42 homolog

This work was funded by the European Research Council (ERC) under the European Union's Horizon 2020 Research and Innovation Programme under grant agreement no. 637614 (NanoPaths). K.Y. was supported by a PhD scholarship from the China Scholarship Council. A.S. would like to acknowledge additional funding from the University of Groningen (Rosalind Franklin Fellowship).

The authors declare no conflicts of interest.

^{*}Corresponding author at: Department of Nanomedicine & Drug Targeting, Groningen Research Institute of Pharmacy, University of Groningen, 9713AV Groningen, The Netherlands.

E-mail address: a.salvati@rug.nl (A. Salvati).

¹ These authors contributed equally to this publication.

<https://doi.org/10.1016/j.nano.2020.102300>

1549-9634/© 2020 The Author(s). Published by Elsevier Inc. This is an open access article under the CC BY license (<http://creativecommons.org/licenses/by/>

both the corona composition and – as a consequence of this – nanocarrier interactions with cells.^{12,18–20}

Overall, in order to reduce protein binding, different strategies have been developed. The most common is the addition of polymers such as polyethylene glycol on the surface of nanocarriers in order to obtain so-called “stealth” surfaces.^{21–23} Interestingly, recent reports have suggested that the stealth character of these nanocarriers is not due to the reduction of protein binding, but by the presence of specific corona proteins adsorbing on PEGylated surfaces.¹⁷ In addition, different strategies are emerging to mask the surface of nanocarriers with “markers of self” to avoid clearance. These include modification with self-peptides such as CD47, and other biomimetic approaches where cell membranes from red blood cells or leukocytes are used to camouflage nanocarriers.^{11,24–26}

Another common strategy to reduce protein binding is the use of zwitterionic modifications. Zwitterionic molecules contain both positive and negative charges, but have a net neutral charge. The introduction of zwitterionic groups on nanocarriers, similar to PEGylation, leads to reduction of protein binding and increased plasma residence time.^{27–29} In line with these results, we have recently shown that by adding increasing amounts of zwitterionic lipids, liposomes with reduced corona binding and lower uptake efficiency by cells could be obtained.³⁰ However, not much is known about the impact of zwitterionic modifications on the mechanisms cells use to internalize nanocarriers in comparison to charged ones. The uptake mechanism can affect nanocarrier uptake efficiency, thus the amount of drug delivered intracellularly, as well as the intracellular processing and final fate of nanocarriers. All of these factors ultimately contribute to the therapeutic efficacy.

Thus, in this work phosphatidylglycerol and phosphatidylcholine, both combined with cholesterol, were used to prepare – respectively – negatively charged and zwitterionic liposomes. Liposomes are very common nanocarriers, usually made with neutral and negatively charged lipids for drug delivery, while positively charged liposomes are widely applied as non-viral gene delivery systems to bind negatively charged nucleic acids.^{31–35} Even though several liposomal formulations have reached the market, not much is known about the effect of charge on the mechanism of liposome uptake by cells. Most studies have investigated the uptake mechanism of positively charged liposomes for nucleic acid delivery.^{36,37} Only a few have directly compared the mechanisms involved in the internalization of zwitterionic and negatively charged liposomes by cells.^{38–40} To this aim, here we have used a panel of common pharmacological inhibitors and RNA interference to block key components of different endocytic pathways on HeLa cells,^{37,41–45} and compared their effect on the uptake of negatively charged and zwitterionic liposomes. This allowed us to determine the effect of zwitterionic modifications on the mechanisms cells use to internalize liposomes.

Methods

Liposome preparation

Lipids were purchased from Avanti Polar Lipids (Alabaster, Alabama, United States). The zwitterionic lipid 1,2-dioleoyl-sn-glycero-3-phosphocholine (DOPC) or the anionic lipid 1,2-

dioleoyl-sn-glycero-3-phospho-(1'-rac-glycerol) (DOPG) were dissolved in chloroform and mixed with cholesterol in a 2:1 molar ratio. Additional experiments were performed with pure DOPC or DOPG liposomes without cholesterol. The solvent was evaporated using nitrogen followed by overnight incubation under vacuum. The lipid films were resuspended in 25 mM sulforhodamine B (SRB) dissolved in phosphate buffered saline (PBS) at room temperature to a final lipid concentration of 10 mg/mL. The suspension was freeze-thawed eight times followed by 21 extrusions through a 0.1 μ m polycarbonate membrane with the Avanti Mini-Extruder (Avanti Polar Lipids). The excess free SRB was removed using Zeba Spin Desalting Columns, 7 K molecular weight cut off (MWCO) (Thermo Fisher Scientific, Waltham, Massachusetts, United States). The liposomes were stored at 4 °C and used for maximum 1 month.

Characterization of liposomes

The hydrodynamic diameter and zeta potential of the liposomes were measured in water, PBS, and Minimum Essential Medium (MEM) (Gibco, Grand Island, New York, United States) supplemented with 4 mg/mL human serum (human serum pooled from multiple donors from TCS Biosciences (Buckingham, United Kingdom)) (hsMEM) using Malvern ZetaSizer Nano ZS (Malvern Instruments, Malvern, United Kingdom). Dynamic and electrophoretic light scattering measurements were performed using 40- μ L cuvettes (Malvern, ZEN0040) and disposable folded capillary cells (Malvern, DTS1070), respectively. Per sample, 3 measurements of 10 runs each were carried out at 25 °C.

Cell culture

Human cervical cancer HeLa cells (CCL-2; ATCC, Manassas, Virginia, United States) were cultured in complete culture medium (cMEM) consisting of MEM supplemented with 10% fetal bovine serum (FBS) (Gibco). The cells were grown in a T75 flask at 37 °C and 5% CO₂ and split when confluent. Cells were tested monthly to exclude mycoplasma contamination and used for experiments till maximum 20 passages after defrosting. The cell culture conditions for A549 and TRP3 cells are described in the Supplementary material.

Isolation of corona-coated liposomes and protein corona characterization

Corona-coated liposomes were isolated by size exclusion chromatography (SEC) and characterized as described in details in the Supplementary material.

Uptake studies and exposure to chemical inhibitors

Different chemical inhibitors were used to block specific components of endocytosis, using previously optimized conditions to ensure drug efficacy and exclude toxicity.⁴⁶ HeLa cells were seeded at a density of 50,000 cells per well in a 24-well plate. Then, 24 h after seeding, cells were pretreated with cMEM containing one of the inhibitors as follows: sodium azide (5 mg/mL) (Merck, Kenilworth, New Jersey, United States) for 30 min, nocodazole (5 μ M) (BioVision Inc., San Francisco, California, United States) for 20 min, or chlorpromazine (10 μ g/mL) (Sigma Aldrich, St. Louis, Missouri, United States), 5-(N-ethyl-N-isopropyl)amiloride (EIPA;

75 μM) (Sigma Aldrich), cytochalasin D (5 $\mu\text{g}/\text{mL}$) (Invitrogen, Carlsbad, California, United States), or methyl- β -cyclodextrin (MBCD, 2.5 mg/mL) (Sigma Aldrich) for 10 min. Then, cells were washed with serum-free medium and incubated with 50 $\mu\text{g}/\text{mL}$ liposomes in MEM supplemented with 4 mg/mL human serum in standard conditions or in the presence of each of the inhibitors. In the case of MBCD, in order to avoid exposure to liposomes in the presence of free proteins which can limit drug efficacy,⁴⁶ HeLa cells were exposed to 50 $\mu\text{g}/\text{mL}$ corona-coated liposomes in serum-free MEM. For this purpose, 0.5 mg/mL liposomes were dispersed in 40 mg/mL human serum for 1 h at 37 °C. The mixed solution was then loaded on a SEC column and the eluted fractions containing liposomes were collected as described in Supplementary material and added to cells to a final lipid concentration of 50 $\mu\text{g}/\text{mL}$ in serum-free MEM. As a control for chlorpromazine, EIPA, and MBCD efficacy, the uptake of – respectively - 1 $\mu\text{g}/\text{mL}$ human low-density lipoprotein labeled with BODIPY (LDL-BODIPY) (Invitrogen) in serum-free MEM, 250 $\mu\text{g}/\text{mL}$ 10 kDa Tetramethylrhodamine dextran (Invitrogen) in cMEM, and 0.1 μM BODIPY-FL-labeled LacCer (Invitrogen) in serum-free MEM was measured in standard conditions or in the presence of the drug. To confirm cytochalasin D and nocodazole efficacy, immunostaining was used as described in details in the Supplementary material.

RNA interference

In order to silence the expression of dynamin-1 and dynamin-2, 13,000 HeLa cells were plated per well of a 24-well plate. Twenty-four hours after seeding, cells were washed with serum-free MEM for 15 min. Oligofectamine-siRNA complexes were formed by mixing 1 μL of Oligofectamine transfection reagent (Life Technologies, Carlsbad, CA, United States) with 10 pmol of siRNA (Thermo Fisher Scientific) against either dynamin-1 (Silencer Select S144) or dynamin-2 (Silencer Select S4213), or scrambled siRNA (Silencer Select negative control no. 1) in 49 μL of OptiMEM. After 20 min incubation at room temperature, the complexes were diluted in serum-free MEM to a total volume of 250 μL , and were added to the cells. After 4 h, MEM supplemented with FBS was added to a final concentration of 10% FBS. Three days after transfection, cells were exposed to either liposomes (50 $\mu\text{g}/\text{mL}$ in MEM supplemented with 4 mg/mL human serum) or – as a control – Alexa Fluor 647-labeled human transferrin (5 $\mu\text{g}/\text{mL}$ in serum-free MEM) (Invitrogen) and their uptake was measured using flow cytometry.

Flow cytometry analysis

After exposure to the liposome or the different controls, cells were washed once with cMEM and twice with PBS to reduce the presence of liposomes or fluorescent probes on the outer cell membrane. Cells were detached by exposure to trypsin/EDTA (0.05% in PBS) for 5 min at 37 °C and collected after centrifugation at 300 g for 5 min. Cells were then resuspended in 100 μL PBS for flow cytometry analysis using a CytoFLEX S (Beckman Coulter, Indianapolis, Indiana, USA). Gates were set in the forward and side scattering plots to exclude cell debris and doublets and at least 10,000 single cells were acquired, unless indicated otherwise. Data were analyzed using FlowJo software (Becton, Dickinson & Company, Ashland, Tennessee, United

States), and the average and standard deviation of the median cell fluorescence intensity over 3 replicates were calculated (unless stated differently).

Fluorescence imaging

To visualize liposome uptake, 1.5×10^5 cells were seeded in 35 mm dishes with a 170 μm thick glass bottom. Twenty-four hours after seeding, cells were washed with serum-free medium and incubated with 50 $\mu\text{g}/\text{mL}$ liposomes in hsMEM for 3 h, followed by lysosome staining with 100 nM LysoTracker Deep Red (Thermo Fisher Scientific) for 30 min and nuclei staining with 1 $\mu\text{g}/\text{mL}$ Hoechst 33342 Solution in cMEM (Thermo Fisher Scientific) for 5 min. Cells were imaged using a DeltaVision Elite microscope (GE Healthcare Life Sciences, Marlborough, Massachusetts, United States) with a DAPI filter for Hoechst excitation, TRITC filter for liposomes, and CY5 filter for LysoTracker. Movies were recorded by acquiring one image every 10 s for up to 3 min for cells exposed to DOPC liposomes (Supplementary Video S1) or 2 min for cells exposed to DOPG liposomes (Supplementary Video S2). Deconvolution was applied using softWoRx 6 acquisition and integrated deconvolution software (GE Healthcare Life Science). Images were further processed using ImageJ software (<http://www.fiji.sc>), and brightness and contrast were adjusted using the same setting for all samples in the series. In order to make the internalized DOPC liposomes visible, an image of the DOPC liposome channel with increased brightness is included for comparison.

Results

Liposome characterization

Liposomes of zwitterionic DOPC or negatively charged DOPG and cholesterol in a 2:1 molar ratio were prepared and labeled by incorporating sulforhodamine B in the hydrophilic core. In order to compare their mechanisms of uptake, human cervical cancer epithelial HeLa cells were selected as a common cell model for similar studies.^{38,41,45,47} Given the strong impact of corona formation on nanoparticle-cell interactions and recognition by cell receptors,^{15,16,45,48} the liposomes were dispersed in a medium supplemented with 4 mg/mL human serum (hsMEM), as opposed to standard fetal bovine serum, in order to allow a human serum corona formation for testing on human cells. Prior to cell studies, the zeta potential and hydrodynamic size of the liposomes in relevant media were determined by electrophoretic and dynamic light scattering (DLS) (Figure 1, A and B). DLS showed that liposomes of comparable size distribution were obtained, with a diameter of approximately 100 nm in PBS and a low polydispersity index and they remained stable once dispersed in medium with human serum (Supplementary Figure S1). The zeta potential of DOPG liposomes in DPBS was strongly negative (-40 ± 3 mV), and was attenuated in hsMEM (-8 ± 1 mV) upon corona formation. The zwitterionic DOPC liposomes in DPBS had a zeta potential close to neutrality (-1 ± 1 mV), which in hsMEM converged to values similar to DOPG liposomes in the same media. We

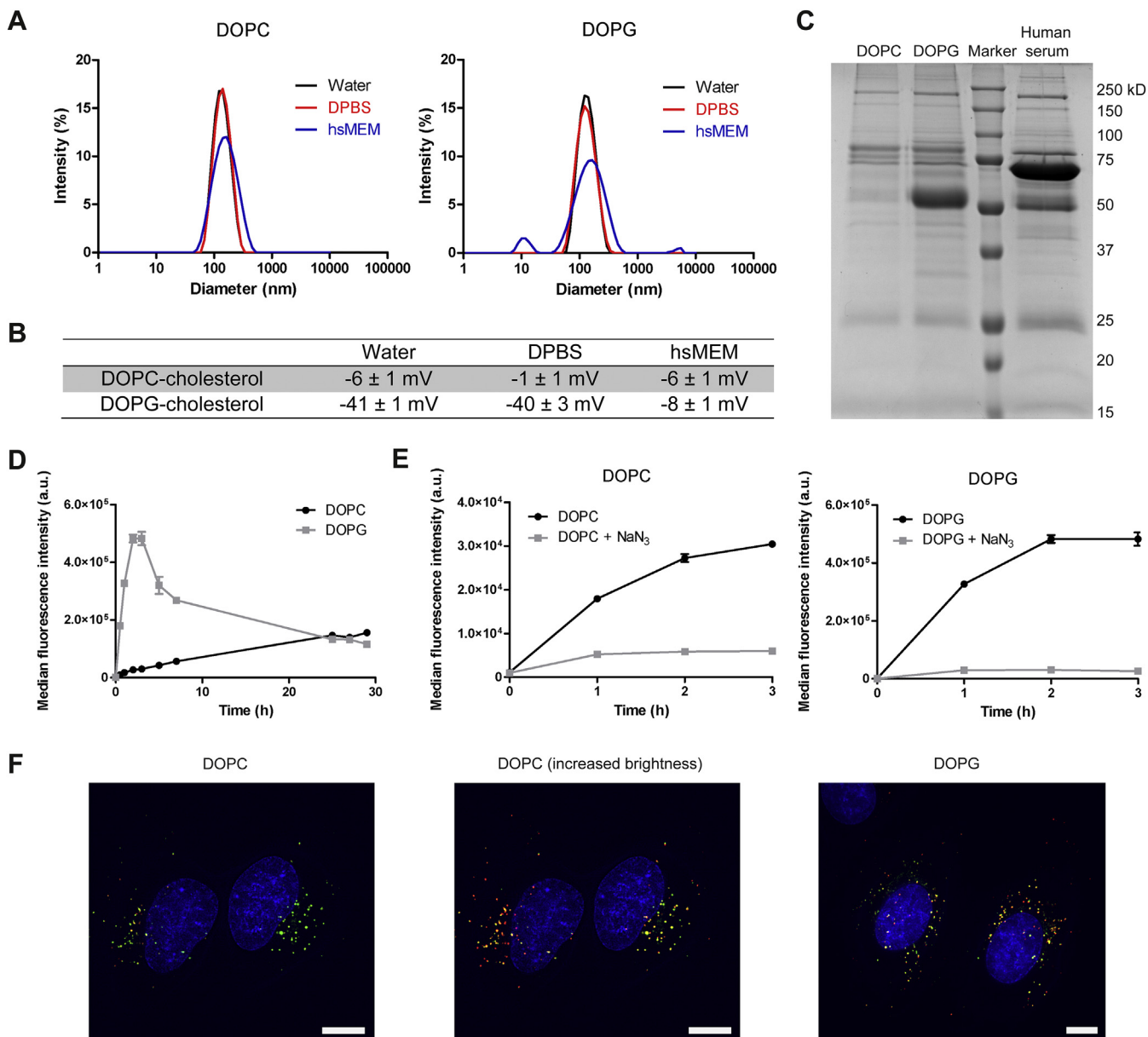


Figure 1. Liposome physicochemical characterization, uptake kinetics and final intracellular location. (A) Size distribution by dynamic light scattering and (B) zeta potential measurements of 50 $\mu\text{g}/\text{mL}$ DOPC and DOPG liposomes in water, PBS, and MEM medium supplemented with 4 mg/mL human serum (hsMEM). (C) Image of an SDS-PAGE gel of the corona proteins recovered from DOPC and DOPG liposomes. Briefly, human serum was first depleted of larger particles and protein aggregates (see Methods for details), thus the corona formed on 75 $\mu\text{g}/\text{mL}$ liposomes in 6 mg/mL particle-depleted human serum was isolated and the recovered proteins isolated by SDS-PAGE. (D-E) Uptake kinetics by HeLa cells of 50 $\mu\text{g}/\text{mL}$ DOPC and DOPG liposomes in hsMEM. In panel E, uptake was measured in standard conditions or in the presence of 5 mg/mL NaN_3 to deplete cell energy. The results are the mean and standard deviation over three technical replicates of the median cell fluorescence intensity obtained by flow cytometry. (F) Fluorescence images of live HeLa cells exposed to 50 $\mu\text{g}/\text{mL}$ liposomes (red) in hsMEM for 3 h. Blue: Hoechst stained nuclei. Green: LysoTracker to stain acidic compartments (scale-bar, 10 μm). In the middle panel, due to the lower uptake efficiency, the brightness of the DOPC channel was increased with Image J to confirm liposome uptake and location. The individual channels of the same images are shown in Supplementary Figure S3 and the corresponding videos are given in Supplementary video S1 and S2.

previously showed that, consistent with their different charge, the DOPG liposomes adsorbed more proteins than the DOPC liposomes, and the resulting corona composition differed strongly, as also confirmed here by SDS-PAGE of the corona proteins in Figure 1, C.³⁰

Uptake kinetics and uptake mechanisms

As a next step, liposome uptake kinetics was determined by flow cytometry. As we previously observed,³⁰ the uptake kinetics of the two formulations differed strongly. Even though multiple liposome

batches with variable fluorescence were used, in all cases DOPG liposomes showed much higher uptake in the first hours, in comparison to the zwitterionic DOPC (Figure 1, D). This is in agreement with previous studies with similar formulations.^{29,49,50} Higher uptake for the DOPG liposomes was observed also when liposomes were added to cells in artificial serum-free conditions, thus when the different charge was not masked by the adsorbed proteins (Supplementary Figure S2).

To determine whether the liposomes entered through an active process or passive fusion with the cell membrane, sodium azide was used to deplete cell energy (Figure 1, E). The very strong reduction of uptake in energy-depleted cells (on average 75 and 90% for DOPC and DOPG liposomes, respectively) indicated that they both entered cells through an energy-dependent mechanism. Live cell imaging confirmed that both liposomes entered the cells and accumulated in the lysosomes (Figure 1, F, Supplementary Figure S3, and corresponding Supplementary videos S1 and S2).

Similar experiments were performed for comparable formulations without cholesterol in the liposome membrane (Supplementary Figure S4): also in this case uptake was higher for the (pure) DOPG liposomes and energy depletion reduced uptake, though the effect was smaller than for liposomes containing cholesterol (40–50% uptake reduction). This suggests that also without cholesterol in the liposome bilayer uptake was at least in part energy-dependent.

As a next step, to characterize the mechanisms of uptake, several key components of endocytic pathways were blocked using a panel of common chemical inhibitors or RNA interference.^{42–44,51} We previously optimized in detail the conditions to use these compounds on HeLa cells in order to exclude toxicity and demonstrate drug efficacy with appropriate controls.⁴⁶ In line with these studies, internalization of fluorescently labeled molecules or fluorescent staining were included in each individual experiment as a control (Figure 2, all left panels). An example of liposome uptake kinetics in standard conditions and in the presence of each of the different compounds tested is given in Figure 2, together with their respective controls. An overview of inhibition efficacy in replicate experiments is included in Figure 3, together with additional studies after cholesterol depletion from the cell membrane.

One of the major pathways of uptake is clathrin-mediated endocytosis (CME). Here, CME was inhibited using chlorpromazine.⁵² The strong reduction of low-density lipoprotein (LDL) uptake confirmed chlorpromazine efficacy (Figures 2, A and 3, A). Interestingly, chlorpromazine reduced the uptake of DOPG liposomes strongly (on average 55% over time), but had no effect on DOPC uptake.

To investigate the role of two major cytoskeleton components, the polymerization of F-actin and microtubules was blocked using cytochalasin D and nocodazole, respectively.^{53,54} As shown in Figure 2, B and C, fluorescence microscopy confirmed the disruption of actin filaments and microtubuli after exposure to these compounds. Cytochalasin D reduced DOPG uptake by 80% after 3 h, but had only a minor effect on DOPC (roughly 30% uptake reduction, as shown in Figures 2, B and 3, B). Similarly, disruption of microtubules with nocodazole reduced DOPG uptake up to a maximum of

50%, while DOPC uptake was less affected (maximum 30% reduction, Figures 2, C and 3, C).

We then tested the involvement of macropinocytosis, an actin-dependent process cells use to internalize extracellular fluids and solutes (Figures 2, D and 3, D). This pathway can be inhibited by amilorides like ethylisopropylamiloride (EIPA) which blocks Na^+/H^+ exchange.⁵⁵ As a control, the uptake of fluorescently labeled dextran was reduced by approximately 60% upon exposure to EIPA. EIPA treatment had clear effects also on the uptake of both liposomes. However, in the case of DOPC liposomes the effect was stronger at increasing exposure time (from 30% after 1 h, up to 60% uptake reduction after 7 h), while for the DOPG liposomes uptake was reduced by 75% already after 1 h (Figures 2, D and 3, D). This suggested that this pathway may be involved in the uptake of both liposomes, but to a different extent. Nonetheless, caution should be taken in interpreting these results, because amilorides block macropinocytosis by lowering the submembranous pH, thereby preventing Rac1 and Cdc42 activation,⁵⁵ which are essential for this mechanism. However, these proteins are involved also in other clathrin-independent endocytic mechanisms.⁵⁶

Another key component for multiple endocytic pathways, including CME, is the GTPase dynamin, involved in the scission of the invaginations from the plasma membrane.⁵⁶ Dynasore is a commonly used inhibitor of dynamin. However, we have previously shown that its activity is lost in medium supplemented with serum.⁴⁶ Thus, RNA interference was used and HeLa cells were transfected with siRNA against DNMI1 or DNMI2 (Figures 2, E and 3, E and Supplementary Figure S5). Silencing DNMI2 had only minor effects on transferrin uptake, which depends on dynamin (Supplementary Figure S5). On the contrary, silencing DNMI1 reduced transferrin uptake by around 60%, confirming efficient silencing (Figure 2, E). DOPC uptake was not affected by silencing of either DNMI1 or DNMI2 (Figures 2, E and 3, E and Supplementary Figure S5, respectively). Instead, for the DOPG liposomes slightly higher uptake was observed after silencing DNMI1 (Figure 2, E), and no clear effects in cells silenced for DNMI2 (only 30% reduction after 1 h, as shown in Supplementary Figure S5). Overall, the absence of effects in cells silenced for DNMI1, for which a clear reduction of transferrin uptake was confirmed, suggested that this protein is not involved in liposome uptake (Figures 2, E and 3, E). Further studies are required to fully elucidate the potential involvement of DNMI2.

Another key component for several endocytic pathways is the cholesterol in the cell membrane (Figure 3F).⁵¹ Cholesterol-dependency is often studied using methyl- β -cyclodextrin (MBCD), which sequesters cholesterol from the cell membrane.⁵¹ However, as for dynasore, we previously showed that this compound loses its efficacy in the presence of serum.⁴⁶ Thus, in order to gain some indications on the potential contribution of cholesterol in the cell membrane to the entry of DOPC and DOPG liposomes into cells, corona-coated liposomes were isolated by size exclusion chromatography, as we previously described.³⁰ Then, the corona-coated liposomes were added to cells in serum-free medium in standard conditions or in the presence of MBCD (Figure 3, F). The uptake of LacCer, a sphingolipid known to enter cells via cholesterol-dependent mechanisms,⁴² was reduced by 65% in cells exposed to MBCD, confirming efficient cholesterol depletion.

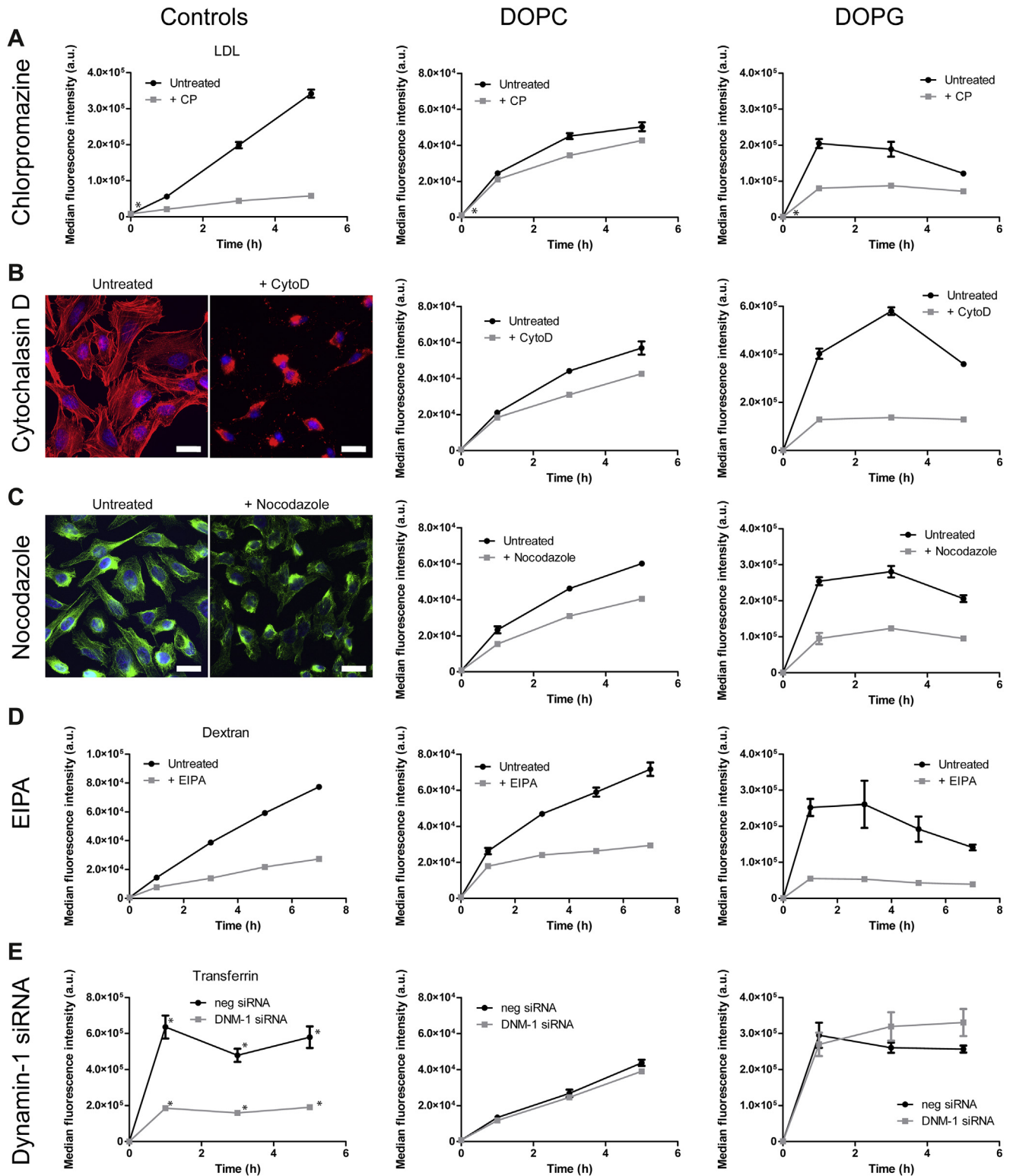


Figure 2. Characterization of the uptake mechanisms of negatively charged and zwitterionic liposomes in HeLa cells. HeLa cells were exposed to DOPC and DOPG liposomes (50 $\mu\text{g}/\text{mL}$) in MEM medium supplemented with 4 mg/mL human serum (hsMEM) in standard conditions (untreated) or in the presence of (A) chlorpromazine (10 $\mu\text{g}/\text{mL}$, CP), (B) cytochalasin D (5 $\mu\text{g}/\text{mL}$, cytoD), (C) nocodazole (5 μM), (D) EIPA (75 μM) or (E) after RNA interference against dynamin-1 (DNM-1 siRNA) (with cells transfected with scrambled RNA, neg siRNA, used as a control, see Methods for details). In the left panels, the uptake of (A) 1 $\mu\text{g}/\text{mL}$ BODIPY-labeled LDL in sfMEM, (D) 250 $\mu\text{g}/\text{mL}$ tetramethylrhodamine-labeled 10 kDa dextran in cMEM, or (E) 5 $\mu\text{g}/\text{mL}$ Alexa Fluor 647-labeled transferrin in sfMEM were used as controls to confirm the effects of the different treatments; while staining of (B) actin and (C) α -tubulin was used to confirm inhibition by cytochalasin D and nocodazole, respectively. The results are the mean and standard deviation over 3 replicate samples (2 replicates for samples marked with *) of the median cell fluorescence intensity obtained by flow cytometry in a representative experiment.

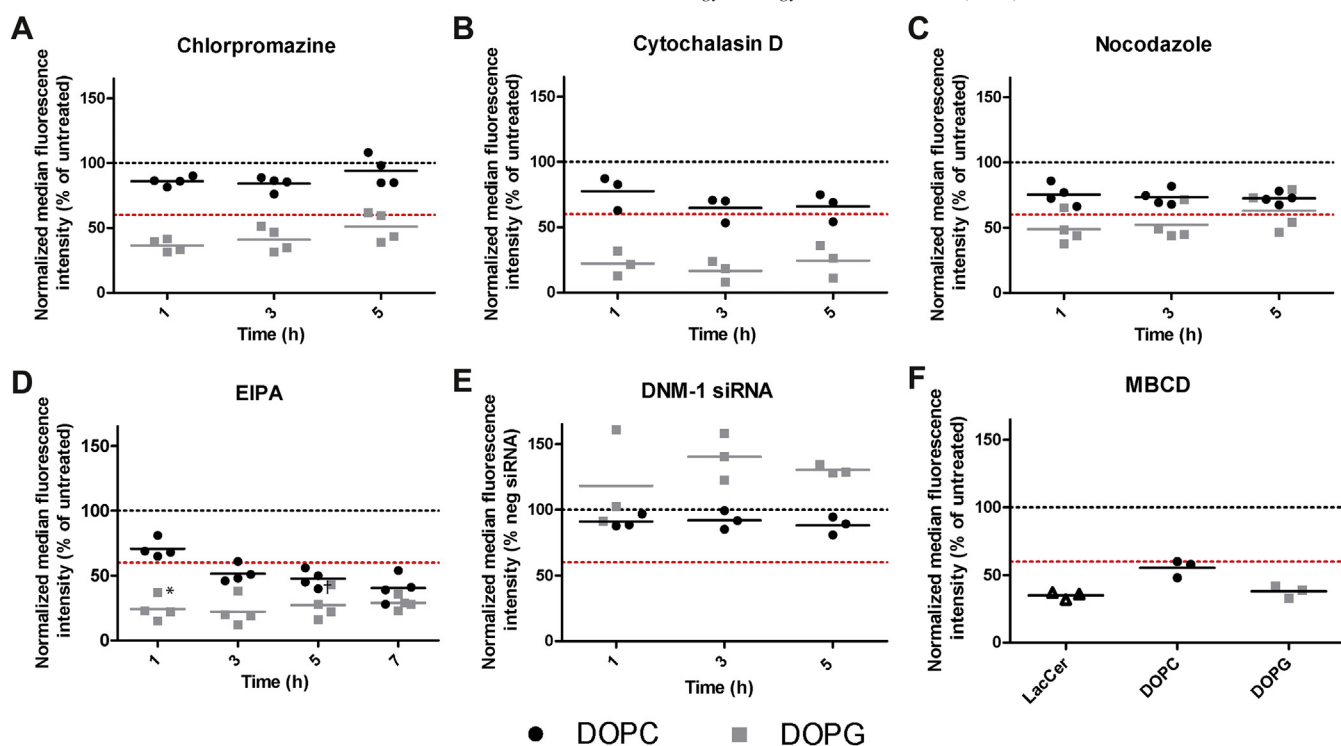


Figure 3. Overview of liposome uptake inhibition in HeLa cells after treatment with the panel of chemical inhibitors or RNA interference. HeLa cells were exposed to DOPC and DOPG liposomes (50 $\mu\text{g}/\text{mL}$) in MEM medium supplemented with 4 mg/mL human serum (hsMEM) in standard conditions or in the presence of (A) chlorpromazine (10 $\mu\text{g}/\text{mL}$), (B) cytochalasin D (5 $\mu\text{g}/\text{mL}$), (C) nocodazole (5 μM), (D) EIPA (75 μM) or (E) after RNA interference against dynamin-1. Additionally, (F) uptake of corona-coated liposomes in sfMEM (50 $\mu\text{g}/\text{mL}$ lipid, isolated as described in the Methods) and, as a control, 0.1 μM BODIPY-FL-labeled LacCer in sfMEM in the presence of methyl- β -cyclodextrin (MBCD, 2.5 mg/mL) was also measured. The symbols are the results obtained in individual experiments (3 to 4 independent replicate experiments) and show the median cell fluorescence intensity averaged over 3 replicate samples (2 replicates for samples marked with *), normalized by the results in untreated control cells. The lines are their average. A black dashed line and a red dashed line are included in each panel as a reference, at 100% and 60% uptake, respectively (with 60% uptake shown as an indicative threshold for inhibition efficacy). In one case, marked with †, for one of the replicate experiments only around 4000 single cells were acquired.

Similarly, cholesterol depletion had strong effects on the uptake of both liposomes (roughly 40% uptake reduction for DOPC and 60% for DOPG, Figure 3, F), suggesting that the cholesterol in the cell membrane plays a role in the entry of both liposomes into HeLa cells.

Similar studies were also performed for comparison in other cell lines, namely human lung cancer A549 epithelial cells and liver endothelial TRP3 cells (Supplementary Figures S6 and S7, respectively).⁵⁹ Also in these cells, DOPG uptake was higher than for DOPC liposomes. In A549 cells, experiments with sodium azide confirmed that uptake was energy-dependent, but none of the inhibitors tested had effects on the uptake of the two liposomes (see details in Supplementary Figure S6). In TRP3 cells, instead, similar to what observed in HeLa (Figures 2 and 3), chlorpromazine and cytochalasin D strongly reduced the uptake of the negatively charged DOPG liposomes, but had only minor or no effect on the uptake of the zwitterionic DOPC. Thus, also in TRP3 cells the two liposomes were internalized via different mechanisms.

Discussion

In this study, the uptake mechanisms of charged and zwitterionic liposomes were compared. Positively charged liposomes are often used to complex and carry oligonucleotides;

however, for drug delivery many of the currently approved liposomal formulations are negatively charged.^{57,58} Thus, here we compared the mechanism of uptake of negatively charged liposomes made with DOPG and zwitterionic DOPC liposomes. Zwitterionic surfaces are known to reduce protein binding and can lead to lower uptake by cells, as indeed we also confirmed here (Figure 1).^{27–30,38,50} However, the effect of zwitterionic modifications on the mechanisms cells use to internalize liposomes has not been fully characterized. The uptake mechanism can affect uptake efficiency, thus the load of drug delivered inside cells, as well as the uptake kinetics, intracellular distribution and final fate of nanocarriers inside cells. All of these aspects, together, ultimately affect drug efficacy, thus it is important to determine how the cell uptake mechanism varies for charged and zwitterionic liposomes. For both liposomes, uptake was energy-dependent (Figure 1, E), excluding some form of passive uptake via direct fusion with the cell membrane. Indeed, the adsorption of the protein corona on the liposomes is likely impairing the possibility for a direct fusion between the lipids of the liposomes and of the cell membrane. Thus, as summarized in Figure 3, blocking a series of key components of the major mechanisms of endocytosis, had very different effects on the uptake of negatively charged and zwitterionic liposomes. In the case of the DOPG liposomes, internalization was reduced by

most inhibitors used, which could suggest the involvement of multiple pathways. Nevertheless, caution should be taken in interpretation of these results, since many of the components investigated (like for instance actin, microtubules, and cholesterol) have a role in multiple endocytic mechanisms and it is known that some of these chemical compounds may influence multiple pathways at the same time.^{42,46,51}

For DOPC liposomes, instead, uptake was clearly clathrin-independent (Figure 3, A), and only cholesterol depletion and treatment with EIPA partially reduced it (Figure 3, D and F, respectively). The latter suggested an involvement of macropinocytosis, however – in contrast with these results – blocking actin polymerization with cytochalasin D did not affect uptake (Figure 3, B). Given that actin is an essential component in macropinocytosis, one may interpret the observed uptake reduction with EIPA as a sign of the involvement of other Rac1 and Cdc42 dependent pathways.⁵⁶ In contrast with our results, Un et al. showed reduced uptake of DOPC-cholesterol liposomes by HeLa cells after inhibition of CME, and no effects when blocking macropinocytosis or after cholesterol depletion.³⁸ The different results may be explained by the different DOPC to cholesterol ratio (1:1 molar ratio, as opposed to 2:1 used in this study) and also by the use of bovine serum instead of human serum for liposome dispersion. It is intriguing to see that small differences in liposome formulation or exposure condition may lead to rather different outcomes at cell level. When performing similar experiments using other cell types, interestingly in A549 cells, none of the inhibitors tested had effects on liposome uptake, even though controls confirmed drug efficacy (Supplementary Figure S6). Other methods need to be applied to understand how the two liposomes are internalized by these cells and eventual differences in the mechanisms used. Instead, in TRP3 cells, similar to what observed in HeLa cells, chlorpromazine and cytochalasin D strongly reduced the uptake of the negatively charged DOPG, but had minor or no effects on the uptake of the zwitterionic DOPC liposomes (Supplementary Figure S7). Thus, also in these cells different mechanisms were used to internalize the two liposomes.

At a broader level, it is interesting to notice that a relatively small difference in the head group of one of the lipids used for the formulation of these liposomes, which otherwise are highly similar (same size, same cholesterol amount, same dioleoyl chains), can have such profound effects not only on the amount and identity of proteins adsorbed once in contact with serum, as well as on uptake efficiency,^{27–30,38,50} but also on the subsequent mechanisms of uptake by cells. Liposome charge itself affects uptake efficiency, as observed when adding the liposomes to cells in artificial serum-free conditions (Supplementary Figure S2), where the different compositions is reflected on the very different zeta potential (as shown in Figure 1, B for liposomes in DPBS). However, cells are unlikely to interact with bare liposomes, since once applied in a biological environment, they are quickly modified by corona formation. In line with this, the zeta potential of the two formulations converged to very similar values upon exposure to serum (also in Figure 1, B). Nevertheless, despite the comparable size and similar charge acquired upon corona formation, liposome uptake efficiency as well as uptake mechanisms differed strongly. This suggests that

for the final corona-coated liposomes, the original charge of the bare liposomes is less relevant in determining the outcomes with cells. Likely, it is the nature and amounts of the proteins adsorbed to determine the strong differences observed in the uptake efficiency and uptake mechanism used by cells to process these apparently similar complexes. In line with this hypothesis, Schöttler et al. have previously reported that the adsorption of clusterin in the corona formed on PEGylated nanocarriers leads to reduced uptake by cells.¹⁷ Similar effects may play a role also in the lower uptake observed for zwitterionic liposomes and it would be interesting to determine which proteins may be responsible for it. Identifying the receptors involved in the higher uptake of the negatively charged DOPG liposomes, as well as potential corona proteins recognized by such receptors, could provide useful information to achieve higher nanocarrier uptake by cells. We have previously shown that recognition by cell receptors of different coronas may lead to different uptake mechanisms by cells and this, in turns, can also affect uptake efficiency and kinetics.⁴⁵ Thus, for efficient drug delivery, the details of the receptors and mechanisms involved in nanocarriers uptake need to be determined, since they can strongly affect delivery efficiency.

These results stress once more that the chemical identity of a nanocarrier alone does not allow predicting its outcomes on cells. Instead, it is the biological identity acquired once nanocarriers are applied in biological environment that modulates interactions with cell receptors, and determines consecutively the mechanism of uptake by cells and uptake efficiency. This is another example suggesting the need for a deeper understanding of the effect of corona formation on the way cells recognize and process nano-sized materials.

Acknowledgments

Imaging has been performed in the Microscopy facility of UMCG in Groningen, the Netherlands. The authors would like to thank Mikhael L. Sowma for his technical assistance in preliminary experiments. Romain Parent and Birke Bartosch (INSERM, Lyon Cancer Research Center, France) are kindly acknowledged for providing the TRP3 cells.

CRediT author statement

Daphne Montizaan: investigation, visualization, formal analysis, writing – original draft;

Keni Yang: Investigation, visualization, formal analysis, writing – review and editing;

Catharina Reker-Smit: Investigation, writing – review and editing;

Anna Salvati: conceptualization, supervision, writing – review and editing.

Appendix A. Supplementary data

Supplementary data to this article can be found online at <https://doi.org/10.1016/j.nano.2020.102300>.

References

- Ferrari M. Cancer nanotechnology: opportunities and challenges. *Nat Rev Cancer* 2005 Mar;**5**(3):161-71.
- Lammers T, Aime S, Hennink WE, Storm G, Kiessling F. Theranostic nanomedicine. *Acc Chem Res* 2011 Oct 18;**44**(10):1029-38.
- Shi J, Kantoff PW, Wooster R, Farokhzad OC. Cancer nanomedicine: progress, challenges and opportunities. *Nat Rev Cancer* 2017 Jan 11;**17**(1):20-37.
- Wilhelm S, Tavares AJ, Dai Q, Ohta S, Audet J, Dvorak HF, et al. Analysis of nanoparticle delivery to tumours. *Nat Rev Mater* 2016 May 26;**1**(5):16014.
- Pelaz B, Alexiou C, Alvarez-Puebla RA, Alves F, Andrews AM, Ashraf S, et al. Diverse applications of nanomedicine. *ACS Nano* 2017 Mar 28;**11**(3):2313-81.
- Venditto VJ, Szoka FC. Cancer nanomedicines: so many papers and so few drugs! *Adv Drug Deliv Rev* 2013 Jan;**65**(1):80-8.
- Monopoli MP, Åberg C, Salvati A, Dawson KA. Biomolecular coronas provide the biological identity of nanosized materials. *Nat Nanotechnol* 2012 Dec 5;**7**(12):779-86.
- Nel AE, Mädler L, Velegol D, Xia T, Hoek EMV, Somasundaran P, et al. Understanding biophysicochemical interactions at the nano-bio interface. *Nat Mater* 2009 Jul 14;**8**(7):543-57.
- Owens DE, Peppas NA. Opsonization, biodistribution, and pharmacokinetics of polymeric nanoparticles. *Int J Pharm* 2006 Jan 3;**307**(1):93-102.
- Moghimi SM, Szebeni J. Stealth liposomes and long circulating nanoparticles: critical issues in pharmacokinetics, opsonization and protein-binding properties. *Prog Lipid Res* 2003 Nov 1;**42**(6):463-78.
- Blanco E, Shen H, Ferrari M. Principles of nanoparticle design for overcoming biological barriers to drug delivery. *Nat Biotechnol* 2015 Sep 8;**33**(9):941-51.
- Aggarwal P, Hall JB, McLeland CB, Dobrovolskaia MA, McNeil SE. Nanoparticle interaction with plasma proteins as it relates to particle biodistribution, biocompatibility and therapeutic efficacy. *Adv Drug Deliv Rev* 2009 Jun;**61**(6):428-37.
- Salvati A, Pitek AS, Monopoli MP, Prapainop K, Bombelli FB, Hristov DR, et al. Transferrin-functionalized nanoparticles lose their targeting capabilities when a biomolecule corona adsorbs on the surface. *Nat Nanotechnol* 2013 Feb 20;**8**(2):137-43.
- Mirshafiee V, Mahmoudi M, Lou K, Cheng J, Kraft ML. Protein corona significantly reduces active targeting yield. *Chem Commun* 2013;**49**(25):2557.
- Lara S, Alnasser F, Polo E, Garry D, Lo Giudice MC, Hristov DR, et al. Identification of receptor binding to the biomolecular Corona of nanoparticles. *ACS Nano* 2017 Feb 28;**11**(2):1884-93.
- Caracciolo G, Cardarelli F, Pozzi D, Salomone F, Maccari G, Bardi G, et al. Selective targeting capability acquired with a protein Corona adsorbed on the surface of 1,2-Dioleoyl-3-trimethylammonium propane/DNA nanoparticles. *ACS Appl Mater Interfaces* 2013 Dec 26;**5**(24):13171-9.
- Schöttler S, Becker G, Winzen S, Steinbach T, Mohr K, Landfester K, et al. Protein adsorption is required for stealth effect of poly(ethylene glycol)- and poly(phosphoester)-coated nanocarriers. *Nat Nanotechnol* 2016 Apr 15;**11**(4):372-7.
- Tenzener S, Docter D, Rosfa S, Wlodarski A, Kuharev J, Rekić A, et al. Nanoparticle size is a critical physicochemical determinant of the human blood plasma Corona: a comprehensive quantitative proteomic analysis. *ACS Nano* 2011 Sep 27;**5**(9):7155-67.
- Walkey CD, Chan WCW. Understanding and controlling the interaction of nanomaterials with proteins in a physiological environment. *Chem Soc Rev* 2012;**41**(7):2780-99.
- Lundqvist M, Stigler J, Elia G, Lynch I, Cedervall T, Dawson K. Nanoparticle size and surface properties determine the protein corona with possible implications for biological impacts. *Proc Natl Acad Sci* 2008 Sep 23;**105**(38):14265-70.
- Otsuka H, Nagasaki Y, Kataoka K. PEGylated nanoparticles for biological and pharmaceutical applications. *Adv Drug Deliv Rev* 2003 Feb 24;**55**(3):403-19.
- Harris JM, Chess RB. Effect of pegylation on pharmaceuticals. *Nat Rev Drug Discov* 2003 Mar;**2**(3):214-21.
- Dai Q, Walkey C, Chan WCW. Polyethylene Glycol Backfilling Mitigates the Negative Impact of the Protein Corona on Nanoparticle Cell Targeting. *Angew Chemie Int Ed*. 2014 Apr 2;**53**(20):n/a-n/a.
- Rodríguez PL, Harada T, Christian DA, Pantano DA, Tsai RK, Discher DE. Minimal "self" peptides that inhibit phagocytic clearance and enhance delivery of nanoparticles. *Science* 2013 Feb 22;**339**(6122):971-5.
- Parodi A, Quattrocchi N, van de Ven AL, Chiappini C, Evangelopoulos M, Martinez JO, et al. Synthetic nanoparticles functionalized with biomimetic leukocyte membranes possess cell-like functions. *Nat Nanotechnol* 2013 Jan 16;**8**(1):61-8.
- Hu CMJ, Zhang L, Aryal S, Cheung C, Fang RH, Zhang L. Erythrocyte membrane-camouflaged polymeric nanoparticles as a biomimetic delivery platform. *Proc Natl Acad Sci* 2011 Jul 5;**108**(27):10980-5.
- Caracciolo G. Liposome-protein corona in a physiological environment: challenges and opportunities for targeted delivery of nanomedicines. *Nanomedicine Nanotechnology, Biol Med* 2015 Apr;**11**(3):543-57.
- García KP, Zarschler K, Barbaro L, Barreto JA, O'Malley W, Spiccia L, et al. Zwitterionic-coated "stealth" nanoparticles for biomedical applications: recent advances in countering biomolecular Corona formation and uptake by the mononuclear phagocyte system. *Small* 2014 Jul;**10**(13):2516-29.
- Safavi-Sohi R, Maghari S, Raoufi M, Jalali SA, Hajipour MJ, Ghassempour A, et al. Bypassing protein Corona issue on active targeting: Zwitterionic coatings dictate specific interactions of targeting moieties and cell receptors. *ACS Appl Mater Interfaces* 2016 Sep 7;**8**(35):22808-18.
- Yang K, Mesquita B, Horvatovich P, Salvati A. Tuning liposome composition to modulate the corona forming in human serum and uptake by cells. *Acta Biomater* 2020 Apr 1;**106**:314-27.
- Weissig V, Pettinger T, Murdock N. Nanopharmaceuticals (part 1): products on the market. *Int J Nanomedicine* 2014 Sep;**9**:4357.
- Barenholz Y. Liposome application: problems and prospects. *Curr Opin Colloid Interface Sci* 2001 Feb 1;**6**(1):66-77.
- Gao X, Huang L. A novel cationic liposome reagent for efficient transfection of mammalian cells. *Biochem Biophys Res Commun* 1991 Aug 30;**179**(1):280-5.
- Miller AD. Cationic liposome systems in gene therapy. *IDrugs* 1998 Sep 3;**1**(5):574-83.
- Allen TM, Cullis PR. Liposomal drug delivery systems: from concept to clinical applications. *Adv Drug Deliv Rev* 2013 Jan;**65**(1):36-48.
- Pichon C, Billiet L, Midoux P. Chemical vectors for gene delivery: uptake and intracellular trafficking. *Curr Opin Biotechnol* 2010 Oct;**21**(5):640-5.
- Li Y, Gao L, Tan X, Li F, Zhao M, Peng S. Lipid rafts-mediated endocytosis and physiology-based cell membrane traffic models of doxorubicin liposomes. *Biochim Biophys Acta - Biomembr* 2016 Aug;**1858**(8):1801-11.
- Un K, Sakai-Kato K, Oshima Y, Kawanishi T, Okuda H. Intracellular trafficking mechanism, from intracellular uptake to extracellular efflux, for phospholipid/cholesterol liposomes. *Biomaterials* 2012 Nov;**33**(32):8131-41.
- Sahay G, Kim JO, Kabanov AV, Bronich TK. The exploitation of differential endocytic pathways in normal and tumor cells in the selective targeting of nanoparticulate chemotherapeutic agents. *Biomaterials* 2010 Feb;**31**(5):923-33.
- Kang JH, Jang WY, Ko YT. The effect of surface charges on the cellular uptake of liposomes investigated by live cell imaging. *Pharm Res* 2017 Apr 11;**34**(4):704-17.
- Dausend J, Musyanovych A, Dass M, Walther P, Schrezenmeier H, Landfester K, et al. Uptake mechanism of oppositely charged fluorescent nanoparticles in HeLa cells. *Macromol Biosci* 2008 Dec 8;**8**(12):1135-43.

42. Vercauteren D, Vandenbroucke RE, Jones AT, Rejman J, Demeester J, De Smedt SC, et al. The use of inhibitors to study Endocytic pathways of gene carriers: optimization and pitfalls. *Mol Ther* 2010 Mar;**18**(3):561-9.
43. Al Soraj M, He L, Peynshaert K, Cousaert J, Vercauteren D, Braeckmans K, et al. siRNA and pharmacological inhibition of endocytic pathways to characterize the differential role of macropinocytosis and the actin cytoskeleton on cellular uptake of dextran and cationic cell penetrating peptides octaarginine (R8) and HIV-tat. *J Control Release* 2012 Jul;**161**(1):132-41.
44. Rejman J, Oberle V, Zuhorn IS, Hoekstra D. Size-dependent internalization of particles via the pathways of clathrin- and caveolae-mediated endocytosis. *Biochem J* 2004 Jan 1;**377**(1):159-69.
45. Francia V, Yang K, Deville S, Reker-Smit C, Nelissen I, Salvati A. Corona composition can affect the mechanisms cells use to internalize nanoparticles. *ACS Nano* 2019 Oct 22;**13**(10):11107-21.
46. Francia V, Reker-Smit C, Boel G, Salvati A. Limits and challenges in using transport inhibitors to characterize how nano-sized drug carriers enter cells. *Nanomedicine* 2019 Jun 18;**14**(12):1533-49.
47. Villanueva A, Cañete M, Roca AG, Calero M, Veintemillas-Verdaguer S, Serna CJ, et al. The influence of surface functionalization on the enhanced internalization of magnetic nanoparticles in cancer cells. *Nanotechnology* 2009 Mar 18;**20**(11):115103.
48. Deng ZJ, Liang M, Monteiro M, Toth I, Minchin RF. Nanoparticle-induced unfolding of fibrinogen promotes mac-1 receptor activation and inflammation. *Nat Nanotechnol* 2011 Jan 19;**6**(1):39-44.
49. Bajoria R, Sooranna SR, Contractor SF. Endocytotic uptake of small unilamellar liposomes by human trophoblast cells in culture. *Hum Reprod* 1997 Jun 1;**12**(6):1343-8.
50. Lee K-D, Hong K, Papahadjopoulos D. Recognition of liposomes by cells: in vitro binding and endocytosis mediated by specific lipid headgroups and surface charge density. *Biochim Biophys Acta - Biomembr* 1992 Jan 31;**1103**(2):185-97.
51. Iversen T-G, Skotland T, Sandvig K. Endocytosis and intracellular transport of nanoparticles: present knowledge and need for future studies. *Nano Today* 2011 Apr;**6**(2):176-85.
52. Wang LH, Rothberg KG, Anderson RGW. Mis-assembly of clathrin lattices on endosomes reveals a regulatory switch for coated pit formation. *J Cell Biol* 1993 Dec 1;**123**(5):1107-17.
53. Flanagan MD, Lin S. Cytochalasins block actin filament elongation by binding to high affinity sites associated with F-actin. *J Biol Chem* 1980 Feb;**255**(3):835-8.
54. Hoebeke J, Van Nijen G, De Brabander M. Interaction of oncodazole (R 17934), a new anti-tumoral drug, with rat brain tubulin. *Biochem Biophys Res Commun* 1976 Mar;**69**(2):319-24.
55. Koivusalo M, Welch C, Hayashi H, Scott CC, Kim M, Alexander T, et al. Amiloride inhibits macropinocytosis by lowering submembranous pH and preventing Rac1 and Cdc42 signaling. *J Cell Biol* 2010 Feb 22;**188**(4):547-63.
56. Sandvig K, Pust S, Skotland T, van Deurs B. Clathrin-independent endocytosis: mechanisms and function. *Curr Opin Cell Biol* 2011 Aug;**23**(4):413-20.
57. Salvioni L, Rizzuto MA, Bertolini JA, Pandolfi L, Colombo M, Prosperi D. Thirty years of Cancer Nanomedicine: success, frustration, and Hope. *Cancers (Basel)* 2019 Nov 25;**11**(12):1855.
58. Chang H-I, Yeh M-K. Clinical development of liposome based drugs: formulation, characterization, and therapeutic efficacy. *Int J Nanomedicine* 2011 Dec;**7**:49.
59. Parent R, Durantel D, Lahlali T, Sallé A, Plissonnier M-L, DaCosta D, Lesca G, Zoulim F, Marion M-J, Bartosch B. An immortalized human liver endothelial sinusoidal cell line for the study of the pathobiology of the liver endothelium. *Biochem Biophys Res Commun* 2014;**450**:7-12.